Chromones bearing amino acid residues: Easily accessible and potent inhibitors of the breast cancer resistance protein ABCG2

Emile Roussel, Alexis Moréno, Nicolas Altounian, Christian Philouze, Basile Pérès, Aline Thomas, Olivier Renaudet, Pierre Falson, Ahcène Boumendjel

Chromones Bearing Amino Acid Residues: Easily Accessible and Potent Inhibitors of the Breast Cancer Resistance Protein ABCG2

Emile Roussel[a,b,c], Alexis Moréno[b], Nicolas Altounian[c], Christian Philouze[c], Basile Pérès[a], Aline Thomas[a], Olivier Renaudet[c], Pierre Falson[b] and Ahcène Boumendjel[a]

[a]Univ. Grenoble Alpes, CNRS, DPM UMR 5063, F-38041 Grenoble, France

[b]Univ. de Lyon 1, CNRS, MMSB UMR 5086, Drug Resistance & Membrane Proteins Lab, 69367 Lyon, France

[c]Univ. Grenoble Alpes, CNRS, DCM UMR 5250, F-38041 Grenoble, France

Keywords: Chromones, BCRP, ABCG2, inhibitors, MDR, drug efflux

Abstract

The Breast Cancer Resistance Protein (BCRP/ABCG2) belongs to the G class of ABC (ATP-Binding Cassette) proteins, which is known as one of the main transporters involved in the multidrug resistance (MDR) phenotype that confer resistance to anticancer drugs. The aim of this study was to design, synthesize and develop new potent and selective inhibitors of BCRP that can be used to abolish MDR and potentialize clinically used anticancer agents. In previous reports, we showed the importance of chromone scaffold and hydrophobicity for the inhibition of ABC transporters. In the present study we report the design and development of chromones linked to one or two amino acids residues that are either hydrophobic or found in the structure of FTC, one of most potent (but highly toxic) inhibitors of BCRP. Herewith, we report the synthesis and evaluation of 13 compounds. The studied molecules were found to be not toxic and showed strong inhibition activity as well as high selectivity toward BCRP. The highest activity was obtained with the chromone bearing a valine residue (**9c**) which showed an inhibition activity against BCRP of 50 nM. The rationalization of the inhibition potential of the most active derivatives was performed through docking studies. Taken together, the ease of synthesis and the biological profile of these compounds render them as promising candidates for further development in the field of anticancer therapy.

1. Introduction

Multidrug resistance (MDR) against anticancer drugs is one of the major causes of chemotherapy failure **[1-3]**. Multidrug resistance (MDR) results in the loss of activity of anticancer agents against cells possessing the MDR phenotype. Multiple mechanisms could be involved in the emergence of MDR, including drug inactivation, target alteration, blockade of apoptosis, stimulation of DNA repair mechanisms and drug efflux **[2,4,5]**. The latter is caused by the overexpression of membrane proteins from the ABC superfamily that export anticancer drugs outside the cell, leading to the reduction of the drug concentration and ultimately decrease the therapeutic effect on cell proliferation.

Three ABC exporters play an important role in the MDR phenotype, P-glycoprotein (ABCB1), MRP1 (ABCC1) and BCRP (ABCG2), which are overexpressed in tumours and therefore are actively studied **[6]**.

BCRP is the most recent discovered ABC human protein **[7-9]**. It is widely expressed in many organs like lungs, gut, liver, placenta and blood-brain barrier **[10,11]**. Moreover, it is naturally overexpressed in stem cells and present in organs responsible for absorption (intestine), elimination (liver and kidney) and distribution of drugs (blood-brain barrier and blood-placental barriers) **[12,13]**. BCRP is a monomer composed of 655 amino acids making it the smallest ABC protein so far reported **[7-9]**. BCRP is one of the ABC proteins that is functional once it is dimerized **[7-9]**. Recently, the 3D structure of human full-length BCRP by electron crystallography or cryo-electron microscopy was reported **[14-16]**.

Over the past three decades, the ABC transporters have been extensively investigated as targets for the development of inhibitors aiming to enhance and restore anticancer drugs potential **[4,17,18]**. In this regard, BCRP was the subject of extensive studies to conceive and develop *in vivo* effective inhibitors to be used as chemosensitizers that could work additively

or synergistically with an anticancer drug **[19-21]**. An important number of *in cellulo* effective inhibitors has been reported but only a few of them were subjected to the preclinical studies **[22]**. Fumitremorgin (FTC) was the first selective inhibitor of ABCG2, which was considered clinically useless because of its high neurotoxicity **[23]**. Nevertheless, it was used an inspiration tool for the development of analogs such as Ko143, less toxic and potent inhibitor **[24, 25]**. Both FTC and Ko143 are strong inhibitors of ABCG2 and composed of fragments found in some amino acids, such as tryptophane, leucine and proline. Otherwise, our previous work on the BCRP/ABCG2 protein led to the development of chromone derivatives as active, selective, nontoxic inhibitors. Among them, the MBL-II-141 (**Figure 1**) has shown promising *in vivo* activity **[19,20,26-28]**.

Based on the structure of MBL-II-141, the importance of hydrophobicity to the inhibition potential and inspired from FTC and Ko143, we focused our present study on chromones bearing one or two hydrophobic amino acids with the aim to develop new class of potent inhibitors that are biological active, non-cytotoxic and specific toward BCRP. The introduction of three amino acids was avoided due anticipated poor solubility that potentially hinder the biological evaluation. Hence, our study targeted 2 series of chromones-embedded amino acids analogues **(Figure 1)**.

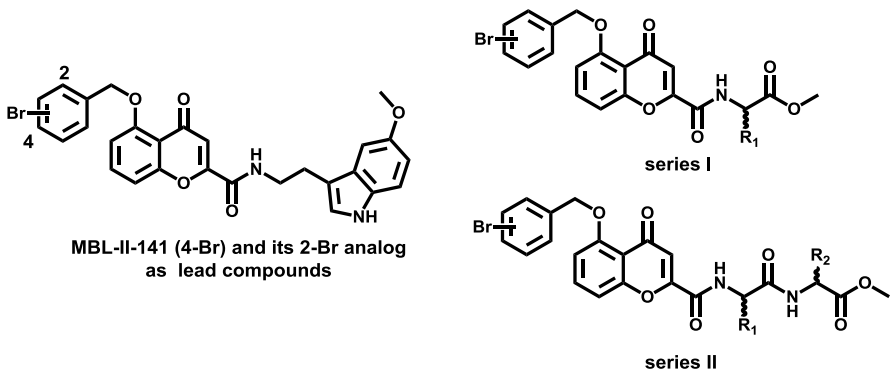

Figure 1. Structure of MBL-II-141 and the general structures of the new series

2. Results and Discussion

2.1. Chemistry

The 2 series of analogues shown in **Figure 1** were synthesized according to the general synthetic pathway described in **Scheme 1**.

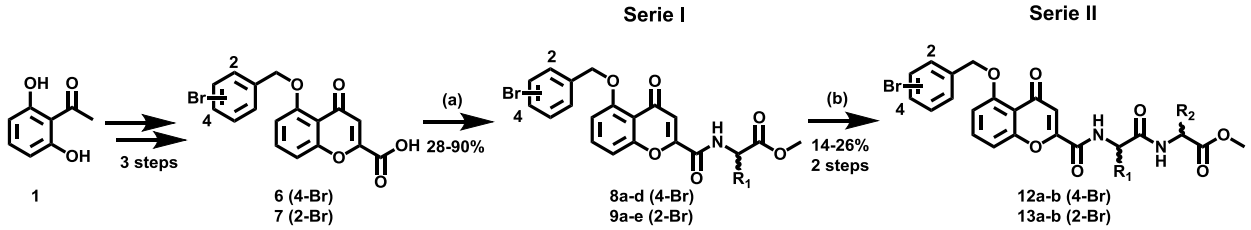

Scheme 1. (**a**) $HCl{\cdot}H_2N\text{-}CH(R_1)\text{-}COOCH_3$, TBTU, DIEA, DMF, RT, 12-24 h; (**b**) **i**- LiOH, $THF/CH_3OH/H_2O$, RT, 2 h; **ii**- $HCl{\cdot}H_2N\text{-}CH(R_2)\text{-}COOCH$, TBTU, DIEA, DMF, RT, 24 h.

The chromone moiety used as the building block for the synthesis of acids **6** and **7** was prepared by adapting our previous described method, using 2,6-dihydroxyacetophenone (**1**), bromobenzyl bromides and ethyl oxalate **[19,29,30]**. An update of the general method is available in the experimental section allowing the synthesis of acids **6** and **7** in several gram scale.

As shown in **Scheme 1**, peptide coupling of chromone derivatives **6** or **7** with protected amino acids was realized in DMF with 2-(1*H*-benzotriazole-1-yl)-1,1,3,3-tetramethylaminium tetrafluoroborate (TBTU) and *N*,*N*-diisopropylethylamine (DIEA) to afford compounds **8a-d** and **9a-c** in yields ranging from 28 to 90 %. Peptide coupling reactions could also be performed by using *N*-Ethyl-*N*′-(3-dimethylaminopropyl)carbodiimide hydrochloride (EDCI,HCl) and 1-hydroxybenzotriazole (HOBt) in the presence of triethylamine or DIEA at room temperature. Overall, the best yields were obtained with TBTU/DIEA **[31-33]**.

The saponification of esters **8a-d** and **9a-e** using lithium hydroxide in a mixture of THF/CH_3OH/H_2O allowed the formation of the corresponding carboxylic acid with 46 - 83 % yields. The second peptide coupling reaction was performed in the same conditions as before to afford compounds **12a-b** and **13a-b** with 31 - 41 % yields. Notably, during this second peptide-coupling reaction we observed a partial racemisation on the asymmetric carbon of the primarily introduced amino acid **[32]**.

Structures of the new compounds were fully elucidated through NMR characterization. In addition, X-ray analysis of **9b** and **9c** confirmed that no racemization had occurred during the first coupling reactions (**Figure 2**). Supplementary data is available on request from the CCDC, 12 Union Road, Cambridge CB2 1EZ, UK, quoting the deposition number CCDC-1874945 and -1874944 for **9b** and **9c** respectively.

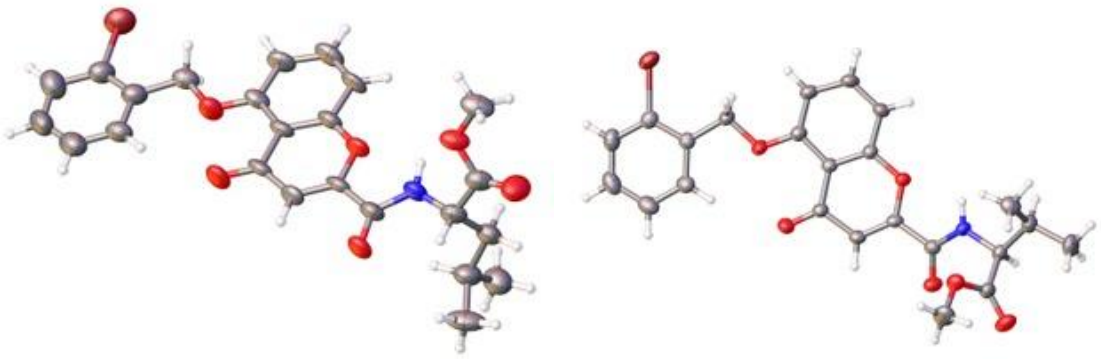

Figure 2. ORTEP schemes for compounds **9b** (left) and **9c** (right) with ellipsoids drawn at the 50% probability level. Atoms were colored as bromide in dark red, oxygen in red, nitrogen in blue, carbon in grey and hydrogen in white.

2.1. ABCG2 inhibition activity and cytotoxicity

The new compounds of the two series were evaluated for their ability to inhibit the efflux of mitoxantrone (MX), an anticancer drug substrate of BCRP that, being fluorescent, can be easily quantified by flow cytometry. The inhibition potency of the compounds was investigated in human embryotic kidney *ABCG2*-transfected cells, HEK293-*ABCG2*, and their

negative control, HEK293 cells. Moreover, the intrinsic cytotoxicity of the compounds was evaluated using the MTT test on the same cell lines. Results are displayed in **Table 1**.

Table 1. Inhibitory activity and cytotoxicity of chromones bearing amino acids residues.

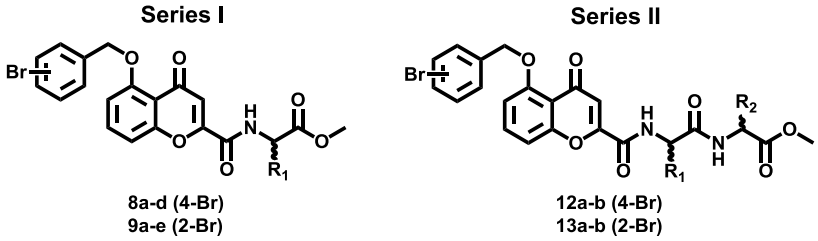

Entry	R_1	R_2	% Maximal inhibition at 1 µM[a]	EC_{50} (µM)	% of Cell viability, at 10-20 µM[b]
8a	(*S*)-CH(CH_3)-CH_2CH_3	/	115 ± 14	0.59 ± 0.08	/
8b	(*S*)-CH_2-Ph	/	92 ± 15	0.27 ± 0.11	84 ± 3
8c	(*S*)-CH_2-(3-indolyl)	/	96 ± 14	0.48 ± 0.07	77 ± 0
8d	(*R*)-CH_2-(3-indolyl)	/	85 ± 12	0.29 ± 0.05	102 ± 1
9a	(*S*)-CH(CH_3)-CH_2CH_3	/	78 ± 9	0.10 ± 0.01	/
9b	(*S*)-CH_2-CH(CH_3)$_2$	/	115 ± 17	0.14 ± 0.04	87 ± 1
9c	(*S*)-CH(CH_3)$_2$	/	87 ± 7	0.05 ± 0.03	76 ± 1
9d	(*S*)-CH_2-Ph	/	100 ± 14	0.10 ± 0.07	82 ± 6
9e	(*S*)-CH_2-(3-indolyl)	/	94 ± 17	0.6 – 0.7	88 ± 1
12a	(*S,R*)-CH(CH_3)-CH_2CH_3	(*S*)-CH(CH_3)$_2$	72 ± 7	0.25 ± 0.1	89 ± 22*
12b	(*S,R*)-CH(CH_3)-CH_2CH_3	(*S*)-CH_2-CH(CH_3)$_2$	52 ± 5	0.11 ± 0.03	101 ± 12*
13a	(*S,R*)-CH(CH_3)-CH_2CH_3	(*S*)-CH(CH_3)$_2$	85 ± 7	0.07 ± 0.01	102 ± 11*
13b	(*S,R*)-CH(CH_3)-CH_2CH_3	(*S*)-CH_2-CH(CH_3)$_2$	83 ± 9	0.07 ± 0.01	104 ± 11*
MBL-II-141	/	/	98 ± 5	0.13 ± 0.09	/
Ko143	/	/	106 ± 1	0.09	/
DMSO 0.5 %					104 ± 8

[a]The percent inhibition of ABCG2 transport activity was studied by comparison with the reference inhibitor Ko143, which fully inhibited; the maximal inhibition for each derivative was measured at 1 mM.
[b]Cytotoxicity was evaluated at 20 µM.
The values of inhibition %, EC_{50} and cell viability are the mean of three independent experiments.

For the series I (compounds bearing one amino acid), the maximal percentage of inhibition at 1 µM of tested compound is close to the references, Ko143 and MBL-II-141. The inhibition activity is stronger with a bromine atom in position 2 (**9a-e**) than in position 4 (**8a-d**) of the benzyloxy group. Such positional effect could be observed by comparing **8a** and **9a**, displaying EC_{50} of ~0.6 vs 0.10 µM, respectively. The importance of stereochemistry of the amino acid is marginal as can be observed with inhibitors **8c** and **8d**. Overall, for this series, the highest activity was reached with compounds **9a-e** for which the hydrophobicity of the amino acid side chain and the position of the bromine atom are beneficial.

For the series II, comparison of compounds **12a-b** and **13a-b** highlighted again the slight contribution of the bromine atom in position 2 of the bromobenzyloxy moiety. Besides, the results obtained with that series also underlined the positive contribution of the second amino acid. The highest inhibitory activity of ABCG2 was obtained with compounds **13a-b** (EC_{50} = 0.07 ± 0.01 µM), regardless the nature of the side chain as long as it is hydrophobic. For comparison purposes, the concentration dependence of mitoxantrone efflux inhibition by Ko143, MBL-II-141 and the two most active compounds (**9c** and **13a**) in HEK293-tranfected cells are provided in the supporting information section.

Taken together, these results highlight the input of the amino acid hydrophobicity on the inhibition of BCRP. It should be highlighted that the introduction of less hydrophobic amino acid was deleterious for the inhibition activity (independent work, results not shown). The position of the bromine atom on the benzyloxy group influences moderately the inhibition activity. Finally, the introduction of a second hydrophobic amino acid is beneficial to reach a high level of ABCG2 inhibition at the expense of low solubility.

The cytotoxicity of chromone derivatives on *ABCG2*-transfected HEK293 cells showed a reliable cell viability for all compounds (**Table 1**). The absence of cytotoxicity prevails an excellent therapeutic index.

2.3. Selectivity toward ABCG2 versus ABCB1 and ABCC1

As introduced above, three exporters are mainly involved in the MDR phenotype, ABCB1, ABCC1 and ABCG2. Hence, we evaluated the selectivity of our compounds by measuring their ability to inhibit the drug efflux mediated by ABCB1 and ABCC1. As shown in **Table 2**, compounds tested at up to 10 µM did not prevent the efflux activity of rhodamine-123 for ABCB1 or calcein for ABCC1, indicating that are selective for ABCG2. More specifically, the five more potent compounds **9b-d** and **13a-b** displayed the highest selectivity at 1 µM and 10 µM.

Table 2. Selectivity of the compounds towards the ABC exporters mainly involved in the MDR phenotype.

Entry	[Compound] (µM)	ABCB1	ABCC1	ABCG2
		% Maximal inhibition at 1 µM		
8b	1	6 ± 2	23.0	92 ± 15
	10	7 ± 1	19.0	/
8c	1	7 ± 3	10.3	96 ± 14
	10	6 ± 1	17.4	/
8d	1	7 ± 1	11.9	85 ± 13
	10	6 ± 1	12.6	/
9a	1	/	5 ± 1	78 ± 9
	10	/	9 ± 5	/
9b	1	7 ± 1	20 ± 3	115 ± 17
	10	5 ± 1	19 ± 2	/
9c	1	8 ± 1	13 ± 1	87 ± 7
	10	7 ± 2	18 ± 1	/
9d	1	5 ± 1	26 ± 1	100 ± 14
	10	6 ± 1	29 ± 2	/
9e	1	7 ± 0	23 ± 3	94 ± 17
	10	5 ± 1	16 ± 3	/

12a	1	2 ± 2	12 ± 0	72 ± 7
	10	11 ± 0	15 ± 2	/
12b	1	4 ± 0	11 ± 1	52 ± 5
	10	6 ± 0	15 ± 1	/
13a	1	0 ± 0	11 ± 1	85 ± 7
	10	0 ± 0	11 ± 3	/
13b	1	2 ± 2	10 ± 1	83 ± 10
	10	2 ± 0	13 ± 1	/

The values of inhibition % are the mean of three independent experiments.

2.4. Interactions of chromone derivatives with the active site of ABCG2

A docking study was successfully achieved using the cryo-EM structure of ABCG2-MZ29-Fab complex (PDB ID: 6HIJ) which contains two MZ29 molecules in the binding site **[16]** (see Supporting Info). For our study, our most active inhibitors (**9c**, **13a** and **13b**), MBL-II-141 and ko143 were docked into the active site of ABCG2 defined as comprising both MZ29 ligands.

Except for ko143, all the ligands best poses adopted a bent configuration that filled both MZ29 binding sites, thanks to the ligand internal flexibilities. The best pose of ligand ko143, a polycyclic and less flexible compound, binds between the two MZ29 binding sites (**Figure 3**).

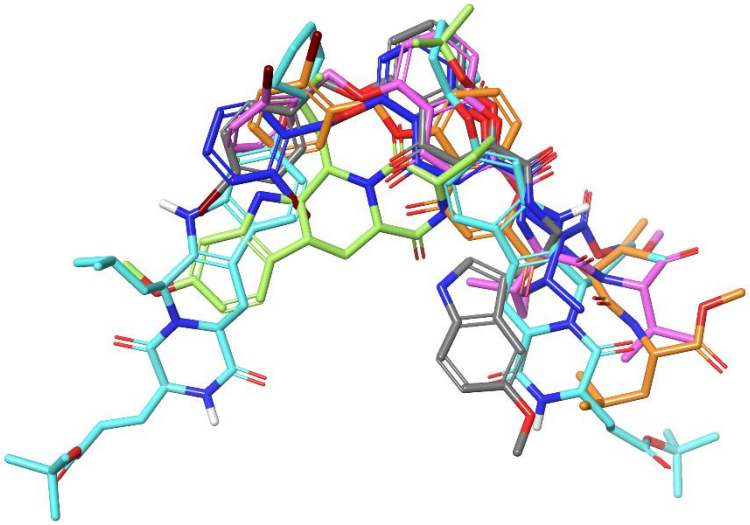

Figure 3. Superposition of the best ranked poses of each ligand on the binding poses of **MZ2**9 colored in cyan, **13a** in purple (-12.5 kcal/mol); **13b** in orange; **MBL-II-141** in grey; **9c** in dark blue (-10.94 kcal/mol) and **ko143** in green (-10.1 kcal/mol).

We observed a large variety of favorable interactions as π - π and hydrophobic interactions which are in agreement with the high docking scores and the inhibition activity determined *in vitro* (**Figure 4**).

The two dipeptides derivatives **13a** and **13b** have small structural difference where only the second amino acid is different (**13a**: (*R*,*S*)-Ile – (*S*)-Val; **13b**: (*R*,*S*)-Ile – (*S*)-Leu). Experimentally as well as by docking, no significant difference of inhibition activity and scores were observed. Note that the racemization that occurs on the first amino acid during the second peptide coupling reaction had no effect on the docking scores.

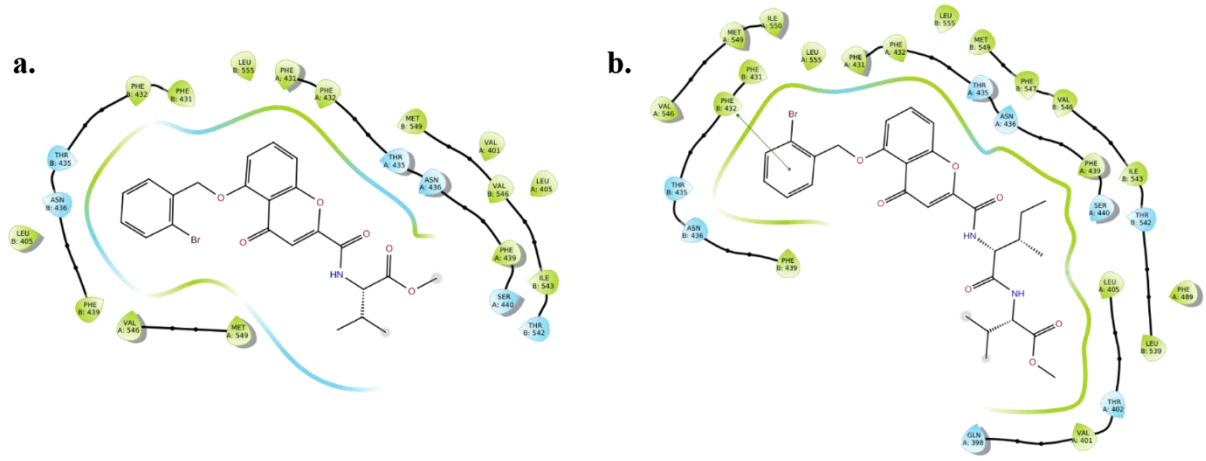

Figure 4. Illustrations of the poses in the binding pocket with respectively in green and cyan, hydrophobic and polar residues. (a) Docking of **9c** in the chosen binding pocket of BCRP. (b) Docking of **13a** in the chosen binding pocket of BCRP.

4. Conclusions

Years ago, we found that conveniently functionalized chromones offer interesting scaffolds for the design of ABCG2 inhibitors. As, the chemistry needed to access chromones scaffolds is now well mastered, it allows the building and refinement of new inhibitors with higher affinity and selectivity. The presence of a carboxylic acid function at the chromone scaffold allows the introduction of amino acid residues through peptidic coupling conditions. The amino acid residues chosen were those found in the FTC and its derivative Ko143, inhibitors. As shown here, chromones bearing one bromine atom in position 2 of the bromobenzyloxy group and a hydrophobic mono- or dipeptide constitute promising leads as inhibitors of drug efflux mediated by ABCG2, being more active than the reference inhibitors Ko143 and MBL-II-141. Their easy chemical synthesis is a key advantage allowing the synthesis of multigram scale quantities of the three more potent compounds **9c**, **13a** and **13b.** The three latter inhibitors are entering in preclinical trials (a patent was filed under the number FR1908485 on September 2019) dealing with the synthesis and inhibition activity of ABCG2 with chromones described in this manuscript. Note that attempts to introduce tripeptides on the

chromone scaffold led to compounds with extreme low solubility that excluded any biological evaluation.

5. Experimental Section

5.1. Chemistry

NMR spectra were recorded on a 400 MHz Bruker Avance-400 instrument (400 MHz) or on a 500 MHz Bruker Avance-500 instrument (500 MHz). Chemical shifts (δ) are reported in ppm relatively to Me_4Si used as an internal standard. Electrospray ionization (ESI) mass spectra were acquired by the Analytical Department of Grenoble University on an Waters Xevo G2-S Q TOF instrument with a nanospray inlet. Exact mass was given in (m/z). HPLC analyses were performed with an Agilent 1100 series using a diode array detector and a C18 reversed-phase column (Nucleosil C18, Macherey-Nagel, 5 mm particle size, 125 mm x 3 mm) at 45 °C, with a mobile phase composed of A: water and TFA 0.1% and B: CH_3OH and TFA 0.1% with a gradient 85:15 to 0:100 A:B over 14 min,1 mL/min, 10 µL injection, detection at 254 nm. Melting point (m.p.) expressed in degrees celsius (°C) were obtained on a Büchi melting point B540. Thin-layer chromatography (TLC) used Merck silica gel F-254 plates (thickness 0.25 mm). Unless otherwise stated, reagents were obtained from commercial sources (Alpha Aesar, Sigma-Aldrich and TCI) and were used without further purification.

Note: The purity of all products is above 95 % and was determined by HPLC or NMR.

5.1.1. General procedures

General procedure A: To a solution of 2,6-dihydroxyacetophenone **1** (1,0 equiv.) in acetone (6 mL/mmol) were added simultaneously K_3CO_3 (3,0 equiv.) and TBAB (0,4 equiv.) previously pounded together. The resulting solution was refluxed during 0.5 or 1 h and then the corresponding bromobenzyl bromide derivative (1,0 equiv.) in acetone (15 mL/mmol) was

added drop by drop under inter atmosphere. The solution was refluxed during 4 or 5 h and monitored by TLC (Cyclohexane/Ethyl acetate 3:7). The solution was concentrated under vacuum and then poured into water before to be extracted with ethyl acetate. The combined organic layers were washed (1 time) with water and brine before dried over magnesium sulfate, filtrated and evaporated under vacuum.

General procedure B: To a solution of **2 or 3** (1.0 equiv.) in dry THF (10 mL/mmol) wad added a solution of sodium ethoxide generated in-situ from sodium metal (6.0 equiv.) in dry ethanol (15 mL/mmol) at 0 °C and under inert atmosphere. Then, the resulting solution was stirred during 30 min at r.t. before to add the diethyl oxalate (4.0 equiv.) drop by drop. The solution was warmed up at 50 °C until precipitation and then refluxed during 2 h and monitored by TLC (Cyclohexane/Ethyl acetate 1:1). Then, few drops of concentrated hydrochloric acid (37 %) were added to the suspension until a white colour change of the precipitate. The resulting suspension was refluxed during 1 h before to be cooled down at r.t. Then, the suspension was concentrated under vacuum and poured into water before to be extracted with ethyl acetate. The combined organic layers were washed (1 time) with water and brine before dried over magnesium sulfate, filtrated and evaporated under vacuum.

General procedure C: To a solution of **4 or 5** (1.0 equiv.) in a combination of THF (25 mL/mmol) and ethanol (8 mL/mmol) was added a solution of K_2CO_3 (1.3 equiv.) in water (12 mL/mmol). Then the resulting solution was warmed up at 50 °C during 4 h and monitored by TLC (Cyclohexane/ethyl acetate 1:1). The solution was concentrated under vacuum and then poured into basified water (K_2CO_3 20 %) and washed with ethyl acetate before to be acidified with HCl 37 %. The aqueous layer was extracted with ethyl acetate or a mixture of dichloromethane with a small amount of THF and methanol Then, the combined organic layers were washed (1 time) with water and brine before dried over magnesium sulfate, filtrated and evaporated under vacuum.

General procedure D: To a solution of **6 or 7** (1.0 equiv.) in dry DMF (20 mL/mmol) was added TBTU (2 equiv.) in the presence of DIEA (4 equiv.) under inert atmosphere. The solution was stirred during 30 min at r.t. Then, a solution of the amino acid methyl ester hydrochloride (2.0 equiv.) in DMF (10 mL/mmol) under inert atmosphere was added to the previous one. The resulting solution was stirred during 12 h to 24 h and monitored by TLC (Cyclohexane/Ethyl acetate 1:1). Then, the solution was concentrated under vacuum and poured into acidified water (HCl 1 M) and extracted with ethyl acetate. The combined organic layers were washed (3 times) with a solution of sodium bicarbonate (20 %). Then, the combined organic layers were washed (1 time) with water and brine before dried over magnesium sulfate, filtrated and evaporated under vacuum.

General procedure D1: To a solution of **10 or 11** (1.0 equiv.) in dry DMF (20 mL/mmol) was added TBTU (2 equiv.) in the presence of DIEA (5 equiv.) under inert atmosphere. The solution was stirred during 30 min at r.t. Then, a solution of the amino acid methyl ester hydrochloride (2.0 equiv.) in DMF (10 mL/mmol) under inert atmosphere was added to the previous one. The resulting solution was stirred during 12 h to 24 h and monitored by TLC (Cyclohexane/Ethyl acetate 3:2). Then, the solution was concentrated under vacuum and poured into acidified water (HCl 1 M) and extracted with ethyl acetate. The combined organic layers were washed (3 times) with a solution of sodium bicarbonate (20 %). Then, the combined organic layers were washed (1 time) with water and brine before dried over magnesium sulfate, filtrated and evaporated under vacuum.

General procedure E: To a solution of **8a or 9a** (1.0 equiv.) in combination of THF (25 mL/mmol) and methanol (10 mL/mmol) was added a solution of LiOH (1.5 equiv.) in H_2O (10 mL/mmol). The resulting solution was stirred 2 h at r.t. and monitored by TLC (Cyclohexane/Ethyl acetate 1:1). Then, the solution was concentrated under vacuum and poured into basified water ($NaHCO_3$ 20 %) and washed (3 times) with ethyl acetate or a

mixture of dichloromethane with a small amount of THF and methanol. The basic aqueous layer was acidified with a solution of hydrochloric acid 1 M, 6 M even concentrated hydrochloridric acid 37 % if needs and extracted with ethyl acetate. Then, the combined organic layers were washed (1 time) with water and brine before dried over magnesium sulfate, filtrated and evaporated under vacuum.

*5.1.2. 1-(2-((4-bromobenzyl)oxy)-6-hydroxyphenyl)ethan-1-one (**2**)*

The crude was synthetized according to the general procedure A starting from **1** (1.500 g, 9.86 mmol). It was purified by a recrystallisation into ethyl acetate to afford **2**, pale yellow crystals (2.321 g, 73 %). $C_{15}H_{13}BrO_3$.

^{1}H NMR (400 MHz, *DMSO-d6*) δ 11.64 (s, 1H), 7.62 – 7.58 (m, 2H), 7.45 – 7.41 (m, 2H), 7.30 (t, *J* = 8.3 Hz, 1H), 6.62 (dd, *J* = 8.4, 0.5 Hz, 1H), 6.52 (dd, *J* = 8.3, 0.7 Hz, 1H), 5.14 (s, 2H), 2.48 (s, 3H). ^{13}C NMR (101 MHz, DMSO-*d6*) δ 203.43, 159.52, 157.94, 135.96, 133.77, 131.41, 129.98, 121.15, 114.75, 109.63, 103.41, 69.30, 33.04. m.p. 114.8 – 116.8 °C. MS (ESI) m/z 320 (^{79}Br), 322 (^{81}Br) $[M]^+$.

*5.1.3. 1-(2-((2-bromobenzyl)oxy)-6-hydroxyphenyl)ethan-1-one (**3**)*

The crude was synthetized according to the general procedure A starting from **1** (1.500 g, 9.86 mmol). It was purified by a recrystallisation into methanol or ethyl acetate to afford **3**, pale yellow crystals (2.583 g, 82 %). $C_{15}H_{13}BrO_3$.

^{1}H NMR (400 MHz, DMSO-*d6*) δ 11.69 (s, 1H), 7.71 (dd, *J* = 8.0, 1.1 Hz, 1H), 7.61 (dd, *J* = 7.6, 1.6 Hz, 1H), 7.46 (m, 1H), 7.39 – 7.29 (m, 2H), 6.67 (dd, *J* = 8.4, 0.5 Hz, 1H), 6.56 (dd, *J* = 8.3, 0.7 Hz, 1H), 5.19 (s, 2H), 2.47 (s, 3H). ^{13}C NMR (101 MHz, DMSO-*d6*) δ 203.38, 159.60, 157.95, 135.31, 133.90, 132.72, 130.64, 130.41, 128.00, 123.04, 114.62, 109.83, 103.19, 70.02, 32.86. m.p. 75.5 – 77.4 °C. MS (ESI) m/z 321 (^{79}Br), 323 (^{81}Br) $[M+H]^+$, 319 (^{79}Br), 321 (^{81}Br) $[M-H]^+$.

*5.1.4. Ethyl 5-((4-bromobenzyl)oxy)-4-oxo-4H-chromene-2-carboxylate (**4**)*

The crude was synthetized according to the general procedure B starting from **2** (1.718 g, 5.35 mmol). It was purified by a recrystallisation into methanol or ethyl acetate to afford **4**, yellow crystals (1.516 g, 70 %). $C_{19}H_{15}BrO_5$.

^{1}H NMR (400 MHz, DMSO-*d6*) δ 7.74 (m, 1H), 7.64 – 7.56 (m, 4H), 7.25 – 7.21 (m, 1H), 7.13 – 7.08 (m, 1H), 6.77 (s, 1H), 5.24 (s, 2H), 4.38 (q, *J* = 7.1 Hz, 2H), 1.34 (t, *J* = 7.1 Hz, 3H). ^{13}C NMR (101 MHz, DMSO-*d6*) δ 176.39, 160.01, 157.70, 157.23, 150.19, 136.23, 135.29, 131.21, 128.90, 120.61, 115.43, 114.68, 110.54, 109.02, 69.22, 62.59, 13.87. m.p. 148.0 – 149.4 °C. MS (ESI) m/z 402 (^{79}Br), 404 (^{81}Br) $[M]^+$.

*5.1.5. Ethyl 5-((2-bromobenzyl)oxy)-4-oxo-4H-chromene-2-carboxylate (**5**)*

The crude was synthetized according to the general procedure B starting from **3** (2.583 g, 8,04 mmol). It was purified by a recrystallisation into methanol or ethyl acetate to afford **5**, yellow crystals (2.478 g, 76 %). $C_{19}H_{15}BrO_5$.

^{1}H NMR (400 MHz, DMSO-*d6*) δ 8.11 (dd, *J* = 7.7, 1.4 Hz, 1H), 7.79 (m, 1H), 7.68 (dd, *J* = 8.0, 1.0 Hz, 1H), 7.51 (m, 1H), 7.33 (m, 1H), 7.30 – 7.25 (m, 1H), 7.18 – 7.13 (m, 1H), 6.79 (s, 1H), 5.23 (s, 2H), 4.40 (q, *J* = 7.1 Hz, 2H), 1.36 (m, 3H). ^{13}C NMR (101 MHz, DMSO-*d6*) δ 176.40, 160.01, 158.25, 157.43, 150.24, 135.70, 135.44, 132.17, 129.57, 129.12, 127.85, 121.05, 115.43, 114.62, 110.78, 108.85, 69.72, 62.61, 13.87. m.p. 155.3 – 157.1 °C. MS (ESI) m/z 403 (^{79}Br), 405 (^{81}Br) $[M-H]^+$.

*5.1.6. 5-((4-bromobenzyl)oxy)-4-oxo-4H-chromene-2-carboxylic acid (**6**)*

The crude was synthetized according to the general procedure C starting from **4** (1.586 g, 3.93 mmol). It was purified by trituration into methanol and then washed with diethyl ether to afford **6**, a white solid (1.259 g, 85 %). It's possible to recrystallize the desired product in methanol to afford white crystal. $C_{17}H_{11}BrO_5$.

^{1}H NMR (400 MHz, DMSO-*d6*) δ 7.76 (m, 1H), 7.66 – 7.59 (m, 4H), 7.24 (dd, *J* = 8.4, 0.7 Hz, 1H), 7.14 – 7.10 (m, 1H), 6.76 (s, 1H), 5.27 (s, 2H). ^{13}C NMR (101 MHz, DMSO-*d6*) δ 176.69, 161.44, 157.69, 157.35, 151.15, 136.27, 135.14, 131.20, 128.89, 120.58, 115.21, 114.69, 110.58, 108.93, 69.23. m.p. 204.6 – 205.3 °C. MS (ESI) m/z 374 (^{79}Br), 376 (^{81}Br) $[M]^{+}$.

*5.1.7. 5-((2-bromobenzyl)oxy)-4-oxo-4H-chromene-2-carboxylic acid (**7**)*

The crude was synthetized according to the general procedure C starting from **5** (1.000 g, 2.48 mmol). It was purified by trituration into methanol and then washed with diethyl ether to afford **7**, a pale yellow solid (0.777 g, 84 %). $C_{17}H_{11}BrO_5$.

^{1}H NMR (400 MHz, DMSO-*d6*) δ 8.14 (dd, *J* = 7.7, 1.1 Hz, 1H), 7.77 (m, 1H), 7.68 (dd, *J* = 8.0, 0.9 Hz, 1H), 7.51 (m, 1H), 7.32 (m, 1H), 7.26 (d, *J* = 8.1 Hz, 1H), 7.13 (d, *J* = 8.3 Hz, 1H), 6.74 (s, 1H), 5.23 (s, 2H). ^{13}C NMR (101 MHz, DMSO-*d6*) δ 176.70, 161.44, 157.42, 157.36, 151.31, 135.75, 135.24, 132.13, 129.52, 129.13, 127.82, 121.01, 115.17, 114.63, 110.80, 108.71, 69.71. m.p. 244.3 °C. MS (ESI) m/z 373 (^{79}Br), 375 (^{81}Br) $[M-H]^{-}$.

*5.1.8. Methyl (5-((4-bromobenzyl)oxy)-4-oxo-4H-chromene-2-carbonyl)-L-alloisoleucinate (**8a**)*

The crude was synthetized according to the general procedure D starting from **6** (0,300 g, 0.80 mmol) and L-isoleucine methyl ester hydrochloride (0,290 g, 1.60 mmol). It was purified by recrystallisation into methanol to afford **8a**, crystals (0.318 g, 79 %). $C_{24}H_{24}BrNO_6$.

^{1}H NMR (400 MHz, *DMSO-d6*) δ 9.17 (d, *J* = 7.9 Hz, 1H), 7.77 (t, *J* = 8.4 Hz, 1H), 7.64 – 7.56 (m, 4H), 7.34 (dd, *J* = 8.5, 0.7 Hz, 1H), 7.12 (d, *J* = 8.1 Hz, 1H), 6.70 (s, 1H), 5.25 (s, 2H), 4.37 (t, *J* = 7.7 Hz, 1H), 3.68 (s, 3H), 2.07 – 1.96 (m, 1H), 1.58 – 1.45 (m, 1H), 1.32 – 1.19 (m, 1H), 0.95 – 0.84 (m, 6H). ^{13}C NMR (101 MHz, *DMSO-d6*) δ 176.41, 171.40, 159.62,

157.63, 157.04, 152.91, 136.29, 134.95, 131.21, 128.92, 120.59, 114.54, 112.73, 110.86, 108.99, 69.19, 57.24, 51.88, 35.48, 25.09, 15.37, 10.77. m.p. 117 °C. HRMS (ESI/QTOF) calcd for $C_{24}H_{25}BrNO_6$ ($M+H^+$) 502.0865, found 502.0853.

5.1.9. Methyl (5-((4-bromobenzyl)oxy)-4-oxo-4H-chromene-2-carbonyl)-L-phenylalaninate ***(8b)***

The crude was synthetized according to the general procedure D starting from **6** (0.472 g, 1.26 mmol) and L-phenylalanine methyl ester hydrochloride (0.453 g, 2.52 mmol). It was purified by recrystallisation into methanol to afford **8b**, crystals (0.551 g, 90 %). $C_{27}H_{22}BrNO_6$.

^{1}H NMR (400 MHz, *DMSO-d6*) δ 9.43 (d, *J* = 7.9 Hz, 1H), 7.79 (t, *J* = 8.4 Hz, 1H), 7.68 – 7.54 (m, 4H), 7.30 (d, *J* = 12.6 Hz, 5H), 7.23 (d, *J* = 6.1 Hz, 1H), 7.13 (d, *J* = 8.3 Hz, 1H), 6.63 (s, 1H), 5.26 (s, 2H), 4.73 (dd, *J* = 13.5, 9.1 Hz, 1H), 3.68 (s, 3H), 3.26 (dd, *J* = 13.8, 5.2 Hz, 1H), 3.16 (dd, *J* = 13.6, 10.3 Hz, 1H). ^{13}C NMR (101 MHz, *DMSO-d6*) δ 176.31, 171.22, 159.22, 157.68, 156.94, 152.71, 137.20, 136.26, 135.08, 131.20, 129.05, 128.91, 128.31, 126.62, 120.59, 114.50, 112.56, 110.60, 109.06, 69.21, 54.10, 52.20, 35.93. m.p. (Decomposition) 153.1 °C. HRMS (ESI/QTOF) calcd $C_{27}H_{23}BrNO_6$ ($M+H^+$) for 536.0709, found 536.0704.

5.1.10. Methyl (5-((4-bromobenzyl)oxy)-4-oxo-4H-chromene-2-carbonyl)-L-tryptophanate ***(8c)***

The crude was synthetized according to the general procedure D starting from **6** (0.100 g, 0.27 mmol) and L-tryptophan methyl ester hydrochloride (0.136 g, 0.533 mmol). It was purified by recrystallisation into methanol to afford **8c**, crystals (0.777 g, 82 %). $C_{29}H_{23}BrN_2O_6$.

^{1}H NMR (400 MHz, *DMSO-d6*) δ 10.90 (s, 1H), 9.34 (d, *J* = 7.8 Hz, 1H), 7.79 (t, *J* = 8.4 Hz, 1H), 7.69 – 7.52 (m, 5H), 7.35 (d, *J* = 8.1 Hz, 1H), 7.29 (d, *J* = 8.1 Hz, 1H), 7.25 (d, *J* = 2.2 Hz, 1H), 7.12 (d, *J* = 8.3 Hz, 1H), 7.10 – 7.03 (m, 1H), 7.02 – 6.94 (m, 1H), 6.63 (s, 1H), 5.25 (s, 2H), 4.80 – 4.69 (m, 1H), 3.68 (s, 3H). Two signals under water peak. ^{13}C NMR (101 MHz, *DMSO-d6*) δ 176.34, 171.50, 159.19, 157.67, 156.92, 152.76, 136.25, 136.10, 135.04, 131.20, 128.92, 127.03, 123.78, 121.02, 120.59, 118.44, 118.04, 114.48, 112.54, 111.48, 110.61, 109.47, 109.06, 69.23, 53.79, 52.18, 26.39. m.p. 235.3 – 236.2 °C. HRMS (ESI/QTOF) calcd for $C_{29}H_{24}BrN_2O_6$ ($M+H^+$) 575.0818, found 575.0807.

5.1.11. Methyl (5-((4-bromobenzyl)oxy)-4-oxo-4H-chromene-2-carbonyl)-D-tryptophanate ***(8d)***

The crude was synthetized according to the general procedure D starting from **6** (0,300 g, 0,80 mmol) and D-tryptophan methyl ester hydrochloride (0.408 g, 1.60 mmol). It was purified by precipitation into ethyl acetate/cyclohexane (2:1) and then washed with diethyl ether to afford **8d**, a pale yellow solid (0.375 g, 81 %). $C_{29}H_{23}BrN_2O_6$.

^{1}H NMR (400 MHz, *DMSO-d6*) δ 10.90 (s, 1H), 9.34 (d, *J* = 7.8 Hz, 1H), 7.79 (t, *J* = 8.4 Hz, 1H), 7.66 – 7.57 (m, 5H), 7.35 (d, *J* = 8.1 Hz, 1H), 7.29 (d, *J* = 8.3 Hz, 1H), 7.25 (d, *J* = 2.1 Hz, 1H), 7.12 (d, *J* = 8.3 Hz, 1H), 7.07 (t, *J* = 7.2 Hz, 1H), 6.98 (t, *J* = 7.4 Hz, 1H), 6.63 (s, 1H), 5.25 (s, 2H), 4.79 – 4.70 (m, 1H), 3.69 (s, 3H), 3.43 – 3.38 (m, 1H), 3.33 – 3.27 (m, 1H). ^{13}C NMR (101 MHz, *DMSO-d6*) δ 176.33, 171.51, 159.18, 157.67, 156.93, 152.75, 136.26, 136.10, 135.04, 131.20, 128.91, 127.03, 123.78, 121.01, 120.59, 118.43, 118.04, 114.48, 112.54, 111.48, 110.60, 109.47, 109.04, 69.21, 53.79, 52.18, 26.38. m.p. 236.2 – 237.9 °C. HRMS (ESI/QTOF) calcd for $C_{29}H_{24}BrN_2O_6$ ($M+H^+$) 575.0818, found 575.0822.

5.1.12. Methyl (5-((2-bromobenzyl)oxy)-4-oxo-4H-chromene-2-carbonyl)-L-alloisoleucinate ***(9a)***

The crude was synthetized according to the general procedure D starting from **7** (0,511 g, 1.36 mmol) and L-isoleucine methyl ester hydrochloride (0.495 g, 2.72 mmol). It was purified by recrystallisation in methanol and then washed with diethyl ether to afford **9a**, crystal, (0.352 g, 51 %). $C_{24}H_{24}BrNO_6$.

^{1}H NMR (400 MHz, *DMSO-d6*) δ 9.23 (d, *J* = 7.7 Hz, 1H), 8.14 (d, *J* = 7.4 Hz, 1H), 7.82 (m, 1H), 7.69 (d, *J* = 7.9 Hz, 1H), 7.52 (m, 1H), 7.40 (d, *J* = 8.4 Hz, 1H), 7.33 (m, 1H), 7.17 (d, *J* = 8.3 Hz, 1H), 6.74 (s, 1H), 5.25 (s, 2H), 4.39 (t, *J* = 7.7 Hz, 1H), 3.70 (s, 3H), 2.10 – 1.99 (m, 1H), 1.60 – 1.48 (m, 1H), 1.33 – 1.23 (m, 1H), 0.97 – 0.86 (m, 6H). ^{13}C NMR (101 MHz, *DMSO-d6*) δ 176.44, 171.41, 159.61, 157.38, 157.05, 152.97, 135.76, 135.11, 132.17, 129.56, 129.14, 127.85, 121.04, 114.49, 112.75, 111.09, 108.81, 69.70, 57.26, 51.90, 35.48, 25.09, 15.37, 10.77. m.p. 123.1 – 125.7 °C. HRMS (ESI/QTOF) calcd for $C_{24}H_{25}BrNO_6$ ($M+H^+$) 502.0865, found 502.0860.

*5.1.13. Methyl (5-((2-bromobenzyl)oxy)-4-oxo-4H-chromene-2-carbonyl)-L-leucinate (**9b**)*

The crude was synthetized according to the general procedure D starting from **7** (0,500 g, 1,33 mmol) and L-leucine methyl ester hydrochloride (0.483 g, 2.66 mmol). It was purified recrystallisation in methanol and then washed with diethyl ether to afford **9b**, a pale yellow solid (0.234 g, 35 %). $C_{24}H_{24}BrNO_6$.

^{1}H NMR (400 MHz, $CDCl_3$) δ 8.13 (d, *J* = 7.4 Hz, 1H), 7.57 (m, 1H), 7.48 (d, *J* = 7.9 Hz, 1H), 7.38 (m, 1H), 7.18 – 7.05 (m, 3H), 6.98 (s, 1H), 6.90 (d, *J* = 8.3 Hz, 1H), 5.18 (s, 2H), 4.82 – 4.73 (m, 1H), 3.74 (s, 3H), 1.80 – 1.60 (m, 3H), 0.99 – 0.87 (m, 6H). ^{13}C NMR (101 MHz, $CDCl_3$) δ 177.52, 172.93, 159.05, 158.46, 157.33, 152.34, 135.55, 134.74, 132.10, 129.07, 128.79, 128.12, 120.82, 115.42, 114.21, 110.63, 108.66, 70.38, 52.73, 51.14, 41.81, 25.02, 22.82, 22.05. m.p. 115.1 – 116.7 °C. HRMS (ESI/QTOF) calcd for $C_{24}H_{25}BrNO_6$ ($M+H^+$) 502.0865, found 502.0865.

*5.1.14. Methyl (5-((2-bromobenzyl)oxy)-4-oxo-4H-chromene-2-carbonyl)-L-valinate (**9c**)*

The crude was synthetized according to the general procedure D starting from **7** (0,200 g, 0,53 mmol) and valine methyl ester hydrochloride (0.179 g, 1.07 mmol). It was purified recrystallisation in methanol and then washed with diethyl ether to afford **9c**, a pale yellow solid (0.126 g, 48 %). $C_{23}H_{22}BrNO_6$.

^{1}H NMR (400 MHz, *DMSO-d6*) δ 9.20 (d, *J* = 7.8 Hz, 1H), 8.12 (d, *J* = 7.4 Hz, 1H), 7.82 (m, 1H), 7.69 (d, *J* = 7.8 Hz, 1H), 7.51 (m, 1H), 7.39 (d, *J* = 8.4 Hz, 1H), 7.33 (m, 1H), 7.16 (d, *J* = 8.3 Hz, 1H), 6.74 (s, 1H), 5.24 (s, 2H), 4.33 (m, 1H), 3.70 (s, 3H), 2.32 – 2.19 (m, 1H), 1.06 – 0.92 (m, 6H). ^{13}C NMR (101 MHz, *DMSO-d6*) δ 176.42, 171.34, 159.69, 157.41, 157.07, 153.03, 135.76, 135.09, 132.17, 129.57, 129.18, 127.84, 121.07, 114.53, 112.74, 111.10, 108.88, 69.76, 58.56, 51.90, 29.46, 19.04, 18.95. m.p. 127.0 – 128.2 °C. HRMS (ESI/QTOF) calcd for $C_{23}H_{23}BrNO_6$ ($M+H^+$) 488.0709, found 488.0719.

*5.1.15. Methyl (5-((2-bromobenzyl)oxy)-4-oxo-4H-chromene-2-carbonyl)-L-phenylalaninate (**9d**)*

The crude was synthetized according to the general procedure D starting from **7** (0,194 g, 0,52 mmol) and L-phenylalanine methyl ester hydrochloride (0.223 g, 1.03 mmol). It was purified by precipitation into ethyl acetate/cyclohexane (2:1) and then washed with diethyl ether to afford **9d**, a pale yellow solid (0.187 g, 70 %). $C_{27}H_{22}BrNO_6$.

^{1}H NMR (400 MHz, *DMSO-d6*) δ 9.47 (s, 1H), 8.13 (dd, *J* = 7.7, 1.5 Hz, 1H), 7.82 (m, 1H), 7.68 (dd, *J* = 8.0, 1.1 Hz, 1H), 7.51 (m, 1H), 7.35 – 7.27 (m, 6H), 7.25 – 7.19 (m, 1H), 7.16 (d, *J* = 8.0 Hz, 1H), 6.64 (s, 1H), 5.24 (s, 2H), 4.77 – 4.71 (m, 1H), 3.69 (s, 3H), 3.26 (dd, *J* = 13.8, 5.4 Hz, 1H), 3.21 – 3.13 (m, 1H). ^{13}C NMR (101 MHz, *DMSO-d6*) δ 176.33, 171.26, 159.21, 157.42, 156.95, 152.77, 137.22, 135.74, 135.24, 132.15, 129.54, 129.11, 129.06, 128.31, 127.84, 126.62, 121.01, 114.43, 112.57, 110.82, 108.85, 69.69, 54.13, 52.20, 30.67. m.p. 145.5 - 147.5 °C. HRMS (ESI/QTOF) calcd for $C_{27}H_{23}BrNO_6$ ($M+H^+$) 536.0709, found 536.0711.

*5.1.16. Methyl (5-((2-bromobenzyl)oxy)-4-oxo-4H-chromene-2-carbonyl)-L-tryptophanate (**9e**)*

The crude was synthetized according to the general procedure D starting from **7** (0,100 g, 0,27 mmol) and L-tryptophan methyl ester hydrochloride (0.137 g, 0.54 mmol). It was purified by precipitation into methanol and then washed with diethyl ether to afford **9e**, a white solid (0.043 g, 28 %). $C_{29}H_{23}BrN_2O_6$.

^{1}H NMR (400 MHz, *DMSO-d6*) δ 10.89 (s, 1H), 9.36 (d, *J* = 7.8 Hz, 1H), 8.12 (d, *J* = 7.7 Hz, 1H), 7.83 (m, 1H), 7.69 (dd, *J* = 8.0, 0.9 Hz, 1H), 7.62 (d, *J* = 7.8 Hz, 1H), 7.51 (m, 1H), 7.39 – 7.28 (m, 3H), 7.25 (d, *J* = 2.2 Hz, 1H), 7.17 (d, *J* = 8.3 Hz, 1H), 7.07 (m, 1H), 6.98 (m, 1H), 6.65 (s, 1H), 5.24 (s, 2H), 4.80 – 4.70 (m, 1H), 3.69 (s, 3H). Two proton signals under water peak ^{13}C NMR (101 MHz, *DMSO-d6*) δ 176.36, 171.52, 159.18, 157.43, 156.95, 152.81, 136.09, 135.74, 135.21, 132.17, 129.57, 129.15, 127.85, 127.03, 123.79, 121.05, 121.02, 118.44, 118.04, 114.43, 112.55, 111.48, 110.83, 109.47, 108.89, 69.73, 53.80, 52.19, 26.38. m.p. 250 – 252.8 °C. HRMS (ESI/QTOF) calcd for $C_{29}H_{24}BrN_2O_6$ ($M+H^+$) 575.0818, found 575.0821.

*5.1.17. (5-((4-bromobenzyl)oxy)-4-oxo-4H-chromene-2-carbonyl)-L-alloisoleucine (**10**)*

The crude was synthetized according to the general procedure E starting from **8a** (0,671 g, 0.51 mmol). It was purified by recrystallisation in methanol and then washed with diethyl ether to afford **10**, white crystals, (0.419 g, 51 %). $C_{23}H_{22}BrNO_6$.

^{1}H NMR (400 MHz, DMSO) δ 12.91 (s, 1H), 8.98 (d, *J* = 8.1 Hz, 1H), 7.78 (m, 1H), 7.67 – 7.57 (m, 4H), 7.37 (dd, *J* = 8.5, 0.6 Hz, 1H), 7.13 (d, *J* = 8.2 Hz, 1H), 6.72 (s, 1H), 5.26 (s, 2H), 4.40 – 4.29 (m, 1H), 2.07 – 1.96 (m, 1H), 1.61 – 1.45 (m, 1H), 1.38 – 1.20 (m, 1H), 0.96 (d, *J* = 6.8 Hz, 3H), 0.90 (t, *J* = 7.4 Hz, 3H). ^{13}C NMR (101 MHz, DMSO) δ 176.44, 172.23, 159.44, 157.63, 157.04, 153.12, 136.28, 134.91, 131.20, 128.93, 120.59, 114.54, 112.63,

110.89, 108.99, 69.21, 57.19, 35.63, 25.04, 15.52, 10.96. m.p. 230.1 – 230.4 °C. HRMS (ESI/QTOF) calcd for $C_{23}H_{23}BrNO_6$ ($M+H^+$) 488.0709, found 488.0715.

*5.1.18. (5-((2-bromobenzyl)oxy)-4-oxo-4H-chromene-2-carbonyl)-L-alloisoleucine (**11**)*

The crude was synthetized according to the general procedure E starting from **9a** (0,256 g, 0.51 mmol). It was purified by recrystallisation into methanol and then washed with diethyl ether to afford **11**, pale yellow crystals, (0.114 g, 46 %). $C_{23}H_{22}BrNO_6$.

^{1}H NMR (400 MHz, *DMSO-d6*) δ 12.91 (s, 1H), 8.98 (d, *J* = 8.1 Hz, 1H), 7.78 (t, *J* = 8.4 Hz, 1H), 7.67 – 7.57 (m, 4H), 7.37 (dd, *J* = 8.5, 0.6 Hz, 1H), 7.13 (d, *J* = 8.2 Hz, 1H), 6.72 (s, 1H), 5.26 (s, 2H), 4.40 – 4.29 (m, 1H), 2.07 – 1.96 (m, 1H), 1.61 – 1.45 (m, 1H), 1.38 – 1.20 (m, 1H), 0.96 (d, *J* = 6.8 Hz, 3H), 0.90 (t, *J* = 7.4 Hz, 3H). ^{13}C NMR (101 MHz, *DMSO-d6*) δ 176.46, 172.23, 159.43, 157.39, 157.06, 153.18, 135.76, 135.07, 132.16, 129.57, 129.16, 127.84, 121.06, 114.49, 112.64, 111.12, 108.84, 69.73, 57.21, 35.62, 25.04, 15.52, 10.96. m.p. 230.1 – 230.4 °C. HRMS (ESI/QTOF) calcd for $C_{23}H_{23}BrNO_6$ ($M+H^+$) 488.0709, found 488.0715.

*5.1.19. Methyl (5-((4-bromobenzyl)oxy)-4-oxo-4H-chromene-2-carbonyl)-L-alloisoleucyl-L-valinate (**12a**)*

The crude was synthetized according to the general procedure D1 starting from **10** (0,123 g, 0.25 mmol) and L-valine methyl ester hydrochloride (0.084 g, 0.50 mmol). It was purified by trituration into diethyl ether to afford **12a**, pale yellow solid, (0.061 g, 41 %). $C_{29}H_{33}BrN_2O_7$.

^{1}H NMR (400 MHz, *DMSO-d6*) δ 8.76 (d, *J* = 8.6 Hz, 0.5H), 8.54 (d, *J* = 9.4 Hz, 1H), 8.43 (d, *J* = 7.5 Hz, 0.5H), 7.76 (t, *J* = 8.3 Hz, 1H), 7.60 (m, 4H), 7.35 (d, *J* = 8.2 Hz, 1H), 7.11 (d, *J* = 8.3 Hz, 1H), 6.69 (d, *J* = 5.4 Hz, 1H), 5.25 (s, 2H), 4.67 (dd, *J* = 8.8, 6.9 Hz, 0.5H), 4.48 (t, *J* = 8.8 Hz, 0.5H), 4.22 (dd, *J* = 7.9, 6.9 Hz, 0.5H), 4.15 (m, 0.5H), 3.63 (d, *J* =

4.9 Hz, 3H), 2.12 – 1.90 (m, 2H), 1.59 – 1.36 (m, 1H), 1.25 – 1.11 (m, 1H), 0.99 – 0.81 (m, 12H). ^{13}C NMR (101 MHz, *DMSO-d6*) δ 176.43, 171.93, 171.64, 170.88, 170.67, 159.10, 158.94, 157.64, 157.01, 153.21, 136.29, 134.90, 131.19, 128.91, 120.58, 114.52, 112.61, 112.54, 110.83, 109.00, 69.21, 57.66, 57.42, 57.24, 56.72, 51.72, 51.53, 37.09, 35.99, 29.85, 29.58, 25.65, 24.62, 19.02, 18.84, 18.35, 18.20, 14.95, 14.58, 11.37, 10.55. m.p. (Decomposition) 268 °C. HRMS (ESI/QTOF) calcd for $C_{29}H_{34}BrN_2O_7$ ($M+H^+$) 601.1549, found 601.1545.

*5.1.20. Methyl (5-((4-bromobenzyl)oxy)-4-oxo-4H-chromene-2-carbonyl)-L-alloisoleucyl-L-leucinate (**12b**)*

The crude was synthetized according to the general procedure D1 starting from **10** (0,123 g, 0.25 mmol) and L-leucine methyl ester hydrochloride (0.091 g, 0.50 mmol). It was purified by trituration into diethyl ether to afford **12b**, pale yellow solid, (0.052 g, 34 %). $C_{30}H_{35}BrN_2O_7$.

^{1}H NMR (400 MHz, *DMSO-d6*) δ 8.76 (d, *J* = 8.7 Hz, 0.5H), 8.62 (d, *J* = 7.8 Hz, 0.5H), 8.54 (dd, *J* = 8.0, 4.5 Hz, 1H), 7.76 (m, 1H), 7.66 – 7.56 (m, 4H), 7.35 (dd, *J* = 8.4, 4.2 Hz, 1H), 7.11 (d, *J* = 8.2 Hz, 1H), 6.70 (d, *J* = 7.5 Hz, 1H), 5.25 (s, 2H), 4.58 (m, 0.5H), 4.39 (m, 0.5H), 4.36 – 4.24 (m, 1H), 3.62 (d, *J* = 2.3 Hz, 3H), 2.03 – 1.89 (m, 1H), 1.70 – 1.55 (m, 2H), 1.55 – 1.45 (m, 2H), 1.24 – 1.10 (m, 1H), 0.96 – 0.79 (m, 12H). ^{13}C NMR (101 MHz, *DMSO-d6)* 176.43, 172.81, 172.60, 170.56, 170.42, 159.14, 158.95, 157.63, 157.01, 153.19, 136.28, 134.90, 131.19, 128.91, 120.57, 114.51, 112.62, 112.54, 110.84, 109.00, 69.20, 57.29, 56.64, 51.86, 51.71, 50.39, 50.23, 36.98, 36.00, 25.59, 24.56, 24.23, 24.18, 22.78, 22.66, 21.28, 20.90, 14.99, 14.62, 10.54. m.p. (Decomposition) 273 °C. HRMS (ESI/QTOF) calcd for $C_{30}H_{36}BrN_2O_7$ ($M+H^+$) 615.1690, found 615.1690.

*5.1.21. Methyl (5-((2-bromobenzyl)oxy)-4-oxo-4H-chromene-2-carbonyl)-L-alloisoleucyl-L-valinate (**13a**)*

The crude was synthetized according to the general procedure D1 starting from **11** (0,091 g, 0.19 mmol) and L-valine methyl ester hydrochloride (0.064 g, 0.38 mmol). It was purified by precipitation into ethyl acetate and a minimum amount of cyclohexane and then washed with diethyl ether to afford **13a**, pale yellow solid, (0.042 g, 37 %). $C_{29}H_{33}BrN_2O_7$.

^{1}H NMR (400 MHz, *DMSO-d6)* δ 8.79 (d, *J* = 8.4 Hz, 0.5H), 8.60 – 8.50 (m, 1H), 8.45 (d, *J* = 7.2 Hz, 0.5H), 8.13 (d, *J* = 7.5 Hz, 1H), 7.81 (m, 1H), 7.69 (d, *J* = 7.8 Hz, 1H), 7.52 (m, 1H), 7.40 (d, *J* = 8.1 Hz, 1H), 7.33 (m, 1H), 7.16 (d, *J* = 8.4 Hz, 1H), 6.72 (d, *J* = 5.0 Hz, 1H), 5.25 (s, 2H), 4.73 – 4.65 (m, 0.5H), 4.54 – 4.45 (m, 0.5H), 4.27 – 4.21 (m, 0.5H), 4.21 – 4.14 (m, 0.5H), 3.65 (d, *J* = 4.7 Hz, 3H), 2.13 – 1.92 (m, 2H), 1.64 – 1.47 (m, 1H), 1.28 – 1.14 (m, 1H), 1.04 – 0.70 (m, 12H).^{13}C NMR (101 MHz, *DMSO-d6*) δ 172.31, 171.91, 171.88, 157.84, 157.83, 157.82, 157.51, 157.49, 157.46, 157.43, 157.42, 153.69, 153.67, 153.65, 135.92, 132.79, 130.34, 129.78, 128.33, 121.94, 114.74, 114.72, 114.70, 114.66, 112.89, 112.87, 112.69, 111.52, 111.46, 109.48, 109.46, 109.37, 109.35, 70.33, 70.31, 58.31, 58.30, 58.21, 58.05, 58.02, 57.96, 52.33, 52.26, 52.23, 52.21, 36.32, 30.00, 25.02, 19.31, 19.17, 19.13, 18.66, 18.59, 15.29, 15.28, 10.85. m.p. (Decomposition) 277 °C. HRMS (ESI/QTOF) calcd for $C_{29}H_{34}BrN_2O_7$ ($M+H^+$) 601.1549, found 601.1533.

*5.1.22. Methyl (5-((2-bromobenzyl)oxy)-4-oxo-4H-chromene-2-carbonyl)-L-alloisoleucyl-L-leucinate (**13b**)*

The crude was synthetized according to the general procedure D1 starting from **11** (0,082 g, 0.16 mmol) and L-leucine methyl ester hydrochloride (0.061 g, 0.32 mmol). It was purified by trituration into diethyl ether to afford **13b**, pale yellow solid, (0.030 g, 31 %). $C_{30}H_{35}BrN_2O_7$.

^{1}H NMR (400 MHz, *DMSO-d6*) δ 8.79 (d, *J* = 8.8 Hz, 0.5H), 8.64 (d, *J* = 7.6 Hz, 1H), 8.56 (d, *J* = 7.7 Hz, 0.5H), 8.13 (d, *J* = 7.6 Hz, 1H), 7.81 (m, 1H), 7.69 (d, *J* = 8.0 Hz, 1H), 7.52 (m, 1H), 7.40 (dd, *J* = 8.3, 4.4 Hz, 1H), 7.33 (m, 1H), 7.16 (d, *J* = 8.1 Hz, 1H), 6.73 (d, *J* = 7.3 Hz, 1H), 5.25 (s, 2H), 4.64 – 4.56 (m, 0.5H), 4.41 (m, 1H), 4.37 – 4.27 (m, 0.5H), 3.63 (s, 3H), 2.05 – 1.92 (m, 1H), 1.74 – 1.43 (m, 4H), 1.27 – 1.13 (m, 1H), 0.98 – 0.81 (m, 12H)). ^{13}C NMR (126 MHz, DMSO-d6) δ 177.64, 174.72, 173.46, 173.29, 171.55, 171.48, 159.81, 159.64, 157.82, 157.41, 153.65, 153.63, 135.89, 135.84, 132.77, 130.31, 129.75, 128.32, 121.89, 114.67, 112.93, 112.88, 111.50, 109.43, 70.31, 58.05, 57.49, 52.53, 52.42, 52.32, 51.52, 51.02, 50.90, 41.57, 40.89, 37.32, 36.39, 25.92, 24.96, 24.70, 24.64, 23.10, 23.01, 22.99, 21.82, 21.57, 21.44, 21.23, 15.31, 14.95, 11.64, 10.85. m.p. (Decomposition) 280 °C. HRMS (ESI/QTOF) calcd for $C_{30}H_{36}BrN_2O_7$ ($M+H^+$) 615.1690, found 615.1684.

5.2. Biology

5.2.1. Materials

DMEM (Dulbecco/Vogt modified Eagle's minimal essential medium) High glucose with GlutaMAX™ (Gibco) and fetal bovine serum (FBS, GE Healthcare Hyclone) were purchased from Fisher Scientific. The penicillin/streptomycin (10 000 unit/10 mg per mL), G418, trypsine and Dulbecco's Phosphate Buffered Saline (DPBS) were purchased from Sigma Aldrich (France) as well as mitoxantrone (MX), rhodamine 123 (R123), calcein AM (cAM) and 3-(4,5-dimethylthiazol-2-yl)-2,5-diphenyl-tetrazolium bromide (MTT). All commercial products were of the highest available purity grade.

5.2.2 Compounds

All chromone derivatives were dissolved in DMSO, and then diluted in DMEM high glucose medium. Stock solutions were stored at -20 °C and warmed to 25 °C just before to use.

5.2.3. Cell lines and cultures

ABCC1-transfected, *ABCB1*-transfected and *ABCG2*-transfected, Flp-In-MDR, NIH/3T3-MDR **[34]** HEK293-MDR **[35]** were obtained as previously published elsewhere **[36]**.

Flp-In293, NIH/3T3 and HEK293 cell lines were cultured and obtained in DMEM-High glucose with GlutaMAX^{TM} supplemented with 10 % heat inactivated FBS and 1 % of penicillin/streptomycin in humidified atmosphere at 37 ºC with 5 % CO_2. In addition, 200 µg/mL hygromycin B, 90 ng/mL colchicine or 750 µg/mL of G418 was added to the growth medium as selection agent for NIH/3T3, Flp-In293 and HEK293 transfected cells respectively. Specifically, for HEK293-MDR the monoclonal cell line was obtained by Fluorescence-Activated Cell Sorting (FACS) using the phycoerythrin-coupled 5D3 antibody (Santa Cruz Biotech) as a native expression reporter.

5.2.4. Cytotoxicity assays

The cytotoxicity of the compounds **8a-d**, **9a-e**, **12a-b** and **13a-b** was determined using a MTT colorimetric assay as reported in literature **[37,38]**. Briefly, cells were seeded into 96-well plates at a density of 1×10^5 cells/well for a total growth medium volume of 100 µL and incubated overnight. Following, 100 µL of fresh medium containing sequential concentrations of compounds to be tested (dissolved in DMSO in a 0, 1 and 10 µM concentration range) were added to each well while DMSO control was fixed at 0.5% (v/v). After 72 h incubation, 22 µL of MTT dye in PBS (5 mg/mL) were added to each well and plates were incubated for an additional 4 h at 37 °C. After medium removal and drying the formazan dye crystals were solubilized with 200 µL of DMSO/ethanol (1:1, v/v). The absorbance was measured using spectrophotometry at 570 nm and 690 nm as reference wavelength. The effect of each compound on cell viability in all cell lines was calculated as the difference in absorbance between test wells and medium control wells.

5.2.5. Inhibition tests of MDR-related drug efflux

Cells were seeded into 96-well plates at a density of 5×10^4 cells/well in 200 µL of medium and incubated overnight. Then, growth medium was switched for fresh medium containing the compounds **8a-d**, **9a-e**, **12a-b** or **13a-b** and in the presence of 4 µM MX as fluorescent probe for BCRP-mediated efflux to a final concentration of 0.5 % DMSO (v/v). After 30 min incubation at 37°C, the medium was removed and cells were washed with 100 µL of DPBS followed by cells dissociation during 5 min at 37°C mediated by 25 µL of trypsin. Finally, trypsin was neutralized with 175 µL of ice-cold DPBS with 2% Bovine Serum Albumin (BSA) and cells were carefully resuspended. As selectivity assay, the same experiment was performed for P-gp- and MRP1-mediated efflux with 0.5 µM R123 or 0.2 µM cAM as respective fluorescent substrates instead of MX.

Intracellular fluorescence was measured with a MacsQuant VRB Analyzer flow cytometer (Miltenyi Biotec) with, at least, 5000 events recorded. While MX was excited at 635 nm and fluorescence emission recorded in a 655-730 nm window, R123 and cAM were excited at 488 nm and recorded in a 525/50 nm filter. The compound inhibition efficacy was estimated by using the following equation:

$$\% \text{ inhibition} = 100 \times \frac{[(G2_{FA} - G2_{FBG}) - (G2_S - G2_{FBG})]}{[(HEK_{FA} - HEK_{FBG}) - (G2_S - G2_{FBG})]}$$

Where $G2_{FA}$ corresponds to the fluorescence emission (a.u.) of accumulated fluorophore in cells expressing the efflux pump incubated with a fluorescent substrate and the tested compound. $G2_{FBG}$ corresponds to the resulting background fluorescence emission (a.u.) in the ABCG2-transfected cells (no substrate and no tested compound). $G2_S$ corresponds to the fluorescence emission (a.u.) of accumulated fluorophore in the cells expressing the efflux pump incubated with the substrate only. HEK_{FA} corresponds to the fluorescence emission (a.u.) of accumulated fluorophore in the control cells incubated with the substrate and the tested compound. HEK_{FBG} corresponds to the resulting background fluorescence emission

(a.u.) in the control cells (no substrate and no tested compound). All values are given as the geometric mean of fluorescence emission (a.u.) in a 655-730 nm filter (excitation 635 nm) measured in 5000 events. Assays were performed in triplicate.

5.2.6. Selectivity assays

NIH/3T3 and Flp-In were seeded into a 96-well plates cells at a density of 5×10^4 cells/well in 200 µL of medium and incubated overnight. Then, growth medium was changed with fresh medium containing the compounds **3a-h** and **4a-c** and in presence of 0.5 µM R123 (NIH/3T3) or 0.2 µM cAM (Flp-In) as fluorescence probe to a final concentration of DMSO 0,5% (v/v). Finally, medium was removed, washed with 100 µL of PBS and cells were trypsinized 5 min at 37°C thanks to 25 µL of trypsin. Then, each medium well was suspended with 175 µL of ice-cold PBS with 2% BSA.

Intracellular fluorescence was measured with a MacsQuant VRB Analyzer flow cytometer (Miltenyi Biotec) with, at least, 5000 events recorded. While MX was excited at 635 nm and fluorescence emission recorded in a 655-730 nm window, R123 and cAM were excited at 488 nm and recorded in a 525/50 nm filter. The compound inhibition efficacy was estimated by using the previous equation. Assays were performed in triplicate.

5.3. Docking

The structure of the ternary complex of human ABCG2 -MZ29–Fab (PDB ID: 6HIJ) was taken as our starting template **[16]**. It was solved by cryo-EM at a resolution of 3.56 Å. The protein exists as a homodimer, and two MZ29 molecules are bound at the central, inward-facing cavity of ABCG2.

We used the Protein Preparation Wizard tool to build an all-atom structure **[39]**. The missing loops of the protein lie beyond 30 Å of the ligands and were thus not considered in the calculations.

The partial atomic charges for the protein and ligand atoms were derived from the OPLS3 force field **[40]**. All the water molecules were retrieved. The histidine residues were treated as neutral. The selection of the histidine enantiomers and the orientation of the asparagine and glutamine side-chains were chosen so as to maximize the hydrogen bond network. An all-atom energy minimization with a 0.3 Å heavy-atom RMSD criteria for termination was performed using the Impref module of Impact and OPLS3 **[41]**.

Low-energy conformers of the chemical compounds, including MZ29, were generated using the LigPrep module. Relevant ionization and tautomeric states at pH comprised between 5 and 9 were generated using the Hammett and Taft methodology implemented in Epik. For compounds available as racemic mixtures, all stereoisomers were generated. The resulting conformations were energy-minimized using OPLS3 force field and a maximum of 32 conformations per ligand were generated and subjected to post-docking minimization **[40].**

The obtained ligands were subjected to a rigid-receptor docking calculation using Glide in Extra Precision mode **[42]**. The shape and physico-chemical properties of the binding site centered on one MZ29 molecule were mapped onto a cubic grid where the innerbox and outerbox have respective dimensions of 18*20*18 and 39*41*39 $Å^3$, thus encompassing both MZ29 binding sites. The hydroxyls of Ser, Thr and Tyr residues were allowed to rotate.

During the docking calculations, the parameters for van der Waals radii were scaled by 0.80 for receptor atoms with partial charges less than 0.15e. A maximum of 100 poses were retained and ranked according to the Glide XP docking scoring function. This docking protocol was able to recover the crystallographic binding pose of MZ29 ligand as the first-

ranked pose with a Glide docking score of -10.26 kcal/mol (see Figures), and RMSD of thus allowing the binding of a second MZ29 ligand in cavity 1. The second-ranked pose of MZ29, with a docking score of -10.23 kcal/mol, shows a slightly titled orientation, which avoids the binding of a second MZ29 ligand in cavity 1. Thus, as debated in the literature (Jackson 2018 and references therein), one cannot state that there is a single or two inhibitors that bind in the protein.

Acknowledgments

This work was supported by CBH-EUR-GS (ANR-17-EURE-0003) to AB and the Ligue Contre le Cancer for PF.

Appendix A. Supplementary data

NMR spectra of the final synthesized compounds (see Experimental Section) are available in a PDF file free of charge.

Crystal structures determinations and refinements details of the compounds **9b** and **9c** are available in a PDF file free of charge.

7. Conflicts of interest

The authors declare no conflicts of interest regarding the publication of this manuscript.

Abbreviations

ABC : ATP Binding Cassette; BBB : Blood–Brain Barrier; BCRP : Breast Cancer Resistance Protein; BSA : bovine Serum Albumin*;* cAM : Calcein Acetoxymethyl; DIEA : N,N-Diisopropylethylamine; DMEM : Dulbecco modified Eagle's minimal essential medium; DMF : Dimethylformamide; EDCI : 1-Ethyl-3-(3-dimethylaminopropyl)carbodiimide; FBS : Fetal Bovine Serum; MDR : Multidrug Resistance ; MRP1 : Multidrug Resistance-associated

protein 1, MTT : 3-(4,5-dimethylthiazol-2-yl)-2,5-diphenyltetrazolium bromide; MX : Mitoxantrone; PAR : Parental; PBS : Phosphate buffered saline; R123 : Rhodamine 123; TBTU : 2-(1H-Benzotriazole-1-yl)-1,1,3,3-tetramethylaminium tetrafluoroborate; THF : Tetrahydrofuran

References

[1] Perez-Tomas, R. Multidrug Resistance: Retrospect and Prospects in Anti-Cancer Drug Treatment. *Curr. Med. Chem.* **2006**, *13* (16), 1859–1876. https://doi.org/10.2174/092986706777585077.

[2] Gillet, J.-P.; Gottesman, M. M. Mechanisms of Multidrug Resistance in Cancer. In *Multi-Drug Resistance in Cancer*; Zhou, J., Ed.; Humana Press: Totowa, NJ, 2010; Vol. 596, pp 47–76. https://doi.org/10.1007/978-1-60761-416-6_4.

[3] Eckford, P. D. W.; Sharom, F. J. ABC Efflux Pump-Based Resistance to Chemotherapy Drugs. *Chem. Rev.* **2009**, *109* (7), 2989–3011. https://doi.org/10.1021/cr9000226.

[4] Chen, Z.; Shi, T.; Zhang, L.; Zhu, P.; Deng, M.; Huang, C.; Hu, T.; Jiang, L.; Li, J. Mammalian Drug Efflux Transporters of the ATP Binding Cassette (ABC) Family in Multidrug Resistance: A Review of the Past Decade. *Cancer Lett.* **2016**, *370* (1), 153–164. https://doi.org/10.1016/j.canlet.2015.10.010.

[5] Pan, S.-T.; Li, Z.-L.; He, Z.-X.; Qiu, J.-X.; Zhou, S.-F. Molecular Mechanisms for Tumour Resistance to Chemotherapy. *Clin. Exp. Pharmacol. Physiol.* **2016**, *43* (8), 723–737. https://doi.org/10.1111/1440-1681.12581.

[6] Borst, P.; Elferink, R. O. Mammalian ABC Transporters in Health and Disease. *Annu. Rev. Biochem.* **2002**, *71* (1), 537–592. https://doi.org/10.1146/annurev.biochem.71.102301.093055.

[7] Allikmets, R.; Schriml, L. M.; Hutchinson, A.; Romano-Spica, V.; Dean, M. A Human Placenta-Specific ATP-Binding Cassette Gene (ABCP) on Chromosome 4q22 That Is Involved in Multidrug Resistance. *Cancer Res.* **1998**, *58* (23), 5337–5339.

[8] Doyle, L. A.; Yang, W.; Abruzzo, L. V.; Krogmann, T.; Gao, Y.; Rishi, A. K.; Ross, D. D. A Multidrug Resistance Transporter from Human MCF-7 Breast Cancer Cells. *Proc. Natl. Acad. Sci. U. S. A.* **1998**, *95* (26), 15665–15670.

[9] Miyake, K.; Mickley, L.; Litman, T.; Zhan, Z.; Robey, R.; Cristensen, B.; Brangi, M.; Greenberger, L.; Dean, M.; Fojo, T. Molecular Cloning of CDNAs Which Are Highly Overexpressed in Mitoxantrone-Resistant Cells. *Cancer Res.* **1999**, *59* (1), 8–13.

[10] Zhou, S.; Schuetz, J. D.; Bunting, K. D.; Colapietro, A.-M.; Sampath, J.; Morris, J. J.; Lagutina, I.; Grosveld, G. C.; Osawa, M.; Nakauchi, H.; et al. The ABC Transporter Bcrp1/ABCG2 Is Expressed in a Wide Variety of Stem Cells and Is a Molecular Determinant of the Side-Population Phenotype. *Nat. Med.* **2001**, *7* (9), 1028–1034. https://doi.org/10.1038/nm0901-1028.

[11] Leslie, E. M.; Deeley, R. G.; Cole, S. P. C. Multidrug Resistance Proteins: Role of P-Glycoprotein, MRP1, MRP2, and BCRP (ABCG2) in Tissue Defense. *Toxicol. Appl. Pharmacol.* **2005**, *204* (3), 216–237. https://doi.org/10.1016/j.taap.2004.10.012.

[12] Tournier, N.; Goutal, S.; Auvity, S.; Traxl, A.; Mairinger, S.; Wanek, T.; Helal, O.-B.; Buvat, I.; Soussan, M.; Caillé, F.; et al. Strategies to Inhibit ABCB1- and ABCG2-Mediated Efflux Transport of Erlotinib at the Blood–Brain Barrier: A PET Study on Nonhuman Primates. *J. Nucl. Med.* **2017**, *58* (1), 117–122. https://doi.org/10.2967/jnumed.116.178665.

[13] Kumar, J. S.; Wei, B.-R.; Madigan, J. P.; Simpson, R. M.; Hall, M. D.; Gottesman, M. M. Bioluminescent Imaging of ABCG2 Efflux Activity at the Blood-Placenta Barrier. *Sci. Rep.* **2016**, *6* (1). https://doi.org/10.1038/srep20418.

[14] Rosenberg, M. F.; Bikadi, Z.; Hazai, E.; Starborg, T.; Kelley, L.; Chayen, N. E.; Ford, R. C.; Mao, Q. Three-Dimensional Structure of the Human Breast Cancer Resistance Protein (BCRP/ABCG2) in an Inward-Facing Conformation. *Acta Crystallogr. D Biol. Crystallogr.* **2015**, *71* (8), 1725–1735. https://doi.org/10.1107/S1399004715010676.

[15] Taylor, N. M. I.; Manolaridis, I.; Jackson, S. M.; Kowal, J.; Stahlberg, H.; Locher, K. P. Structure of the Human Multidrug Transporter ABCG2. *Nature* **2017**. https://doi.org/10.1038/nature22345.

[16] Jackson, S. M.; Manolaridis, I.; Kowal, J.; Zechner, M.; Taylor, N. M. I.; Bause, M.; Bauer, S.; Bartholomaeus, R.; Bernhardt, G.; Koenig, B.; et al. Structural Basis of Small-Molecule Inhibition of Human Multidrug Transporter ABCG2. *Nat. Struct. Mol. Biol.* **2018**, *25* (4), 333–340. https://doi.org/10.1038/s41594-018-0049-1.

[17] Lisa Iorio, A.; da Ros, M.; Fantappiè, O.; Lucchesi, M.; Facchini, L.; Stival, A.; Becciani, S.; Guidi, M.; Favre, C.; de Martino, M.; et al. Blood-Brain Barrier and Breast Cancer Resistance Protein: A Limit to the Therapy of CNS Tumors and Neurodegenerative Diseases. *Anticancer Agents Med. Chem.* **2016**, *16* (7), 810–815. https://doi.org/10.2174/1871520616666151120121928.

[18] Hida, K.; Kikuchi, H.; Maishi, N.; Hida, Y. ATP-Binding Cassette Transporters in Tumor Endothelial Cells and Resistance to Metronomic Chemotherapy. *Cancer Lett.* **2017**, *400*, 305–310. https://doi.org/10.1016/j.canlet.2017.02.006.

[19] Pires, A. do R. A.; Lecerf-Schmidt, F.; Guragossian, N.; Pazinato, J.; Gozzi, G. J.; Winter, E.; Valdameri, G.; Veale, A.; Boumendjel, A.; Di Pietro, A.; et al. New, Highly Potent and Non-Toxic, Chromone Inhibitors of the Human Breast Cancer Resistance Protein ABCG2. *Eur. J. Med. Chem.* **2016**, *122*, 291–301. https://doi.org/10.1016/j.ejmech.2016.05.053.

[20] Honorat, M.; Guitton, J.; Gauthier, C.; Bouard, C.; Lecerf-Schmidt, F.; Peres, B.; Terreux, R.; Gervot, H.; Rioufol, C.; Boumendjel, A.; et al. MBL-II-141, a Chromone Derivative, Enhances Irinotecan (CPT-11) Anticancer Efficiency in ABCG2-Positive Xenografts. *Oncotarget* **2014**, *5* (23), 11957–11970. https://doi.org/10.18632/oncotarget.2566.

[21] Hasanabady, M. H.; Kalalinia, F. ABCG2 Inhibition as a Therapeutic Approach for Overcoming Multidrug Resistance in Cancer. *J. Biosci.* **2016**, *41* (2), 313–324. https://doi.org/10.1007/s12038-016-9601-5.

[22] Wiese, M. BCRP/ABCG2 Inhibitors: A Patent Review (2009–Present). *Expert Opin. Ther. Pat.* **2015**, *25* (11), 1229–1237. https://doi.org/10.1517/13543776.2015.1076796.

[23] Rabindran, S. K.; He, H.; Singh, M.; Brown, E.; Collins, K. I.; Annable, T.; Greenberger, L. M. Reversal of a Novel Multidrug Resistance Mechanism in Human Colon Carcinoma Cells by Fumitremorgin C. *Cancer Res.* **1998**, *58* (24), 5850–5858.

[24] van Loevezijn, A.; Allen, J. D.; Schinkel, A. H.; Koomen, G. J. Inhibition of BCRP-Mediated Drug Efflux by Fumitremorgin-Type Indolyl Diketopiperazines. *Bioorg. Med. Chem. Lett.* **2001**, *11* (1), 29–32. https://doi.org/10.1016/s0960-894x(00)00588-6.

[25] Allen, J. D.; van Loevezijn, A.; Lakhai, J. M.; van der Valk, M.; van Tellingen, O.; Reid, G.; Schellens, J. H. M.; Koomen, G.-J.; Schinkel, A. H. Potent and Specific Inhibition of the Breast Cancer Resistance Protein Multidrug Transporter in Vitro and in Mouse Intestine by a Novel Analogue of Fumitremorgin C. *Mol. Cancer Ther.* **2002**, *1* (6), 417–425.

[26] Hénin, E.; Honorat, M.; Guitton, J.; Di Pietro, A.; Payen, L.; Tod, M. Pharmacokinetic Interactions in Mice between Irinotecan and MBL-II-141, an ABCG2 Inhibitor: Irinotecan MBLI-II-141 Interaction. *Biopharm. Drug Dispos.* **2017**. https://doi.org/10.1002/bdd.2069.

[27] Valdameri, G.; Genoux-Bastide, E.; Peres, B.; Gauthier, C.; Guitton, J.; Terreux, R.; Winnischofer, S. M. B.; Rocha, M. E. M.; Boumendjel, A.; Di Pietro, A. Substituted Chromones as Highly Potent Nontoxic Inhibitors, Specific for the Breast Cancer Resistance Protein. *J. Med. Chem.* **2012**, *55* (2), 966–970. https://doi.org/10.1021/jm201404w.

[28] Winter, E.; Lecerf-Schmidt, F.; Gozzi, G.; Peres, B.; Lightbody, M.; Gauthier, C.; Ozvegy-Laczka, C.; Szakacs, G.; Sarkadi, B.; Creczynski-Pasa, T. B.; et al. Structure–Activity Relationships of Chromone Derivatives toward the Mechanism of Interaction with and Inhibition of Breast Cancer Resistance Protein ABCG2. *J. Med. Chem.* **2013**, *56* (24), 9849–9860. https://doi.org/10.1021/jm401649j.

[29] Reis, J.; Gaspar, A.; Milhazes, N.; Borges, F. Chromone as a Privileged Scaffold in Drug Discovery: Recent Advances: Miniperspective. *J. Med. Chem.* **2017**, *60* (19), 7941–7957. https://doi.org/10.1021/acs.jmedchem.6b01720.

[30] Gaspar, A.; Matos, M. J.; Garrido, J.; Uriarte, E.; Borges, F. Chromone: A Valid Scaffold in Medicinal Chemistry. *Chem. Rev.* **2014**, *114* (9), 4960–4992. https://doi.org/10.1021/cr400265z.

[31] Montalbetti, C. A. G. N.; Falque, V. Amide Bond Formation and Peptide Coupling. *Tetrahedron* **2005**, *61* (46), 10827–10852. https://doi.org/10.1016/j.tet.2005.08.031.

[32] Al-Warhi, T. I.; Al-Hazimi, H. M. A.; El-Faham, A. Recent Development in Peptide Coupling Reagents. *J. Saudi Chem. Soc.* **2012**, *16* (2), 97–116. https://doi.org/10.1016/j.jscs.2010.12.006.

[33] Han, S.-Y.; Kim, Y.-A. Recent Development of Peptide Coupling Reagents in Organic Synthesis. *Tetrahedron* **2004**, *60* (11), 2447–2467. https://doi.org/10.1016/j.tet.2004.01.020.

[34] Pastan, I.; Gottesman, M. M.; Ueda, K.; Lovelace, E.; Rutherford, A. V; Willingham, M. C. A Retrovirus Carrying an MDR1 CDNA Confers Multidrug Resistance and Polarized

Expression of P-Glycoprotein in MDCK Cells. *Proc Natl Acad Sci U A* **1988**, *85* (12), 4486–4490. https://doi.org/10.1073/pnas.85.12.4486.

[35] Robey, R. W.; Honjo, Y.; Morisaki, K.; Nadjem, T. A.; Runge, S.; Risbood, M.; Poruchynsky, M. S.; Bates, S. E. Mutations at Amino-Acid 482 in the ABCG2 Gene Affect Substrate and Antagonist Specificity. *Br J Cancer* **2003**, *89* (10), 1971–1978. https://doi.org/10.1038/sj.bjc.6601370.

[36] Arnaud, O.; Koubeissi, A.; Ettouati, L.; Terreux, R.; Alamé, G.; Grenot, C.; Dumontet, C.; Di Pietro, A.; Paris, J.; Falson, P. Potent and Fully Noncompetitive Peptidomimetic Inhibitor of Multidrug Resistance P-Glycoprotein. *J Med Chem* **2010**, *53* (18), 6720–6729. https://doi.org/10.1021/jm100839w.

[37] Mosmann, T. Rapid Colorimetric Assay for Cellular Growth and Survival: Application to Proliferation and Cytotoxicity Assays. *J Immunol Methods* **1983**, *65* (1–2), 55–63. https://doi.org/10.1016/0022-1759(83)90303-4.

[38] Berridge, M.; Tan, A.; McCoy, K.; Wang, R. The Biochemical and Cellular Basis of Cell Proliferation Assays That Use Tetrazolium Salts. *Biochemica* **1996**, No. 4, 4–9.

[39] Madhavi Sastry, G.; Adzhigirey, M.; Day, T.; Annabhimoju, R.; Sherman, W. Protein and Ligand Preparation: Parameters, Protocols, and Influence on Virtual Screening Enrichments. *J Comput Aided Mol Des* **2013**, *27* (3), 221–234. https://doi.org/10.1007/s10822-013-9644-8.

[40] Harder, E.; Damm, W.; Maple, J.; Wu, C.; Reboul, M.; Xiang, J. Y.; Wang, L.; Lupyan, D.; Dahlgren, M. K.; Knight, J. L.; et al. OPLS3: A Force Field Providing Broad Coverage of Drug-like Small Molecules and Proteins. *J. Chem. Theory Comput.* **2016**, *12* (1), 281–296. https://doi.org/10.1021/acs.jctc.5b00864.

[41] Banks, J. L.; Beard, H. S.; Cao, Y.; Cho, A. E.; Damm, W.; Farid, R.; Felts, A. K.; Halgren, T. A.; Mainz, D. T.; Maple, J. R.; et al. Integrated Modeling Program, Applied

Chemical Theory (IMPACT). *J Comput Chem* **2005**, *26* (16), 1752–1780. https://doi.org/10.1002/jcc.20292.

[42] Friesner, R. A.; Banks, J. L.; Murphy, R. B.; Halgren, T. A.; Klicic, J. J.; Mainz, D. T.; Repasky, M. P.; Knoll, E. H.; Shelley, M.; Perry, J. K.; et al. Glide: A New Approach for Rapid, Accurate Docking and Scoring. 1. Method and Assessment of Docking Accuracy. *J. Med. Chem.* **2004**, *47* (7), 1739–1749. https://doi.org/10.1021/jm0306430.